A Case Study of Double Ridges of Subtropical High over the Western North Pacific: The Role in the 1998 Second Mei-yu over the Yangtze River Valley

Rui-Fen ZHAN

Shanghai Typhoon Institute of China Meteorological Administration, Shanghai, China
State Key Laboratory of Numerical Modeling for Atmospheric Sciences and Geophysical Fluid Dynamics (LASG), Institute of Atmospheric Physics, Chinese Academy of Sciences, Beijing, China

Jian-Ping LI

State Key Laboratory of Numerical Modeling for Atmospheric Sciences and Geophysical Fluid Dynamics (LASG), Institute of Atmospheric Physics, Chinese Academy of Sciences, Beijing, China

Jin-Hai HE and Li QI

Key Laboratory of Meteorological Disaster of Jiangsu Province, Nanjing University of Information Science & Technology, Nanjing, China

(*Manuscript received 23 March 2005, in final form 1 November 2007*)

Abstract

Double ridges in the Western North Pacific Subtropical High (WPSH) in 1998 are studied as a particular case using NCEP/NCAR reanalysis data and the Black Body Temperature (TBB) data. In contrast to typical single ridge in WPSH, double ridges are found during July in 1998 and associated with the second Meiyu activity in the Yangtze River valley. The second ridge of WPSH is built up in the south of the first one and contributes to the stagnancy of WPSH in the south in middle of July. It is different from the previous view that the stagnancy of WPSH in the south resulted from the sudden southward withdrawal of the original ridge.

The characteristics of double ridges including the structure, evolution and possible mechanisms are investigated with the case of 1998. The results show that there are a lot of differences in the large-scale circulation, temperature and humidity between the single ridge and double ridges of the WPSH. The north branch of the double ridges has coherent characteristics with the traditional single ridge, while the south branch is characterized by the tropical systems. There are evidences to support that the formation of the double ridges is associated with the northward movement of equatorial buffer zone and the persistence is related to the evolution of tropical convections.

The rainfall pattern in eastern China associated with the double ridges of WPSH is examined using the instrumental records of precipitation in China. Two rain belts shaped as an italic "L"-like pattern in eastern China are found to be related to the double ridges. This study provides new evidence to understand the variability of WPSH and associated East Asian summer monsoon activity on synoptic scales.

Corresponding author: Jianping Li, LASG, Institute of Atmospheric Physics, Chinese Academy of Sciences, P.O. Box 9804, Beijing 100029, China
E-mail: ljp@lasg.iap.ac.cn

1. Introduction

The Western North Pacific Subtropical High (hereafter, WPSH) is one of the most important components of the East-Asian monsoon system (Tao and Chen 1987). Its meridional shift has a large impact on the location and intensity of the large-scale summer monsoon rainfall over East Asia, identified as Mei-yu or Plum rain in China, Baiu in Japan, and Changma in Korea (Tao and Chen 1987; Ding 1994; Ninomiya 2004). It is well known that a subtropical front associated with Meiyu or Baiu and Changma is found at about the 5°–8° north of the ridge of the WPSH (e.g., Wang et al. 2000). Generally the WPSH jumps twice northwards from winter to summer in the most years (Huang and Tang 1962; Krishnamurti 1979), while the movement of the WPSH is quite complicated with unusual activities in summer such as abrupt jump, stable persistence or withdrawal from the north. In most years, these unexpected activities of the WPSH play an important role in generating the droughts and floods in the east of Asian regions (Ninomiya 1984; Tao and Chen 1987; Wang and Li 2004). For example, the well documented floods over the Yangtze-Huai River Valley of China [Huai River, (31°–36°N, 112°–121°E)] during the 1991 Meiyu season were closely relative to the persistent stagnancy of WPSH in the north compared to its climatological position (Wang et al. 2000). As a link between the tropics and mid-latitudes, the subtropical high (SH) strongly influences the weather and climate systems in both its sides while there is also a reaction from tropical and mid-latitude systems. There are evidences to support that not only the circulation patterns in mid- and high latitudes (Tao and Zhu 1964) but also tropical convection, typhoons, and equatorial anticyclones (Fujita 1969; Sadler 1971; Kurihara 1989; Huang et al. 2004) could have effects on the SH meridional shift.

Single ridge of SH has been emphasized in most of the previous studies, while double ridges as an interesting phenomenon have received less attention. As early as 20 years ago, Sadler (1975) found that there were double ridges over the North Pacific and the North Atlantic at 200 hPa in a climatological study of the upper troposphere. Further analysis shows that such a double-ridge phenomenon could also occur over other regions. On July 11, 1998, for example, two ridges visibly emerge at 500 hPa over East Asia–West Pacific

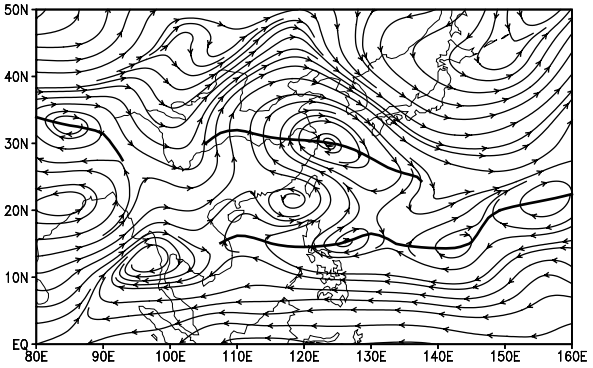

Fig. 1. 500 hPa stream field on July 11, 1998. The thick solid lines denote the ridges of subtropical high (SH).

subtropical latitudes, with one branch in the north (30°N) and the other in the south (15°N) (Fig. 1). Here, it is defined as a double-ridge event extending Sadler's definition. We also notice it appears in almost every year using the NCEP/NCAR reanalysis data and the European Center for Medium-Range Weather Forecasts (ECMWF) reanalysis data. However, there is little published work about this phenomenon and double ridges of subtropical high (hereafter SHDRs) are poorly understood though they could associate with the monsoon activity in East Asia.

The summer of 1998 witnessed extreme rainstorms over the mid-lower valley of the Yangtze River, which is outstanding in all historical records. 223 million people were homeless and over 3600 people died, and property damage was reported up to $32 billion (Gerald et al. 1999; Ding and Liu 2001). Among the various causes of the floods, the abrupt southward withdrawal of WPSH ridge in middle July was regarded as a dominant factor (China National Climate Center 1998; Ding et. al. 2001). Due to close relationship between the ridge of the WPSH and the location of the Mei-yu front, the persistence of ridge at the south of 20°N after the normal Mei-yu period determines the unusual second Mei-yu period and heavy rainfall over the Yangtze River basin, which finally results in the severe floods in 1998. However, we note the SHDRs in the interval between the first and second Mei-yu periods, which is related to the surrounding circulations. This SHDR event lasts 6 days, and its end is followed by the southward stagnancy of WPSH. The SHDR event seems a precursor signal for the onset of the second Mei-

yu that is linked with the southward stagnancy of WPSH. This study will therefore describe the concept of SHDRs, investigate its role in triggering the second Mei-yu in 1998, and explore the possible reason for its formation. These observational results will provide a new understanding for the variability of the WPSH on synoptic scales and its influence on the rainfall.

This paper is organized into 6 sections including the introduction as the first one. The data and methodology are described in the next section. Section 3 presents a new concept–the SHDRs, analyzes some basic circulation features and temperature/humidity structures related to the WPSH double-ridge process in July 1998, and discusses its possible influence on the second Mei-yu event over the mid-lower valleys of the Yangtze River. The generation and development of the double-ridge process are discussed in Section 4. Section 5 investigates possible effect of the double-ridge persistence on the rainfall pattern in central and eastern China. Summary and discussion are given in Section 6.

2. Data and methodology

2.1 Data

The three main datasets are employed in this study. One is the National Centers for Environmental Prediction/National Center for Atmospheric Research (NCEP/NCAR) reanalysis data (Kalnay et al. 1996), particulary the daily conventional data at 12-level standard isobaric surfaces in July, 1998, with 2.5° latitude and 2.5° longitude, and variables include geopotential height ϕ, zonal wind u, meridional wind v, vertical velocity ω, temperature T, relative humidity RH. The second dataset is the daily black body temperatures (TBB) data with the resolution of 0.5° latitude and 0.5° longitude, which is provided by the Meteorological Research Institute of the Japan Meteorological Agency. The last one is the daily precipitation data at 740 stations provided by the China Meteorological Administration.

2.2 The formulation of the WPSH ridge

The quasi-geostrophic equilibrium relation is a fundamental property of large-scale atmospheric motions over extratropics, that is, horizontal pressure gradient force is roughly in balance with horizontal Coriolis force. It is shown from data diagnosis that the large-scale atmospheric motions at lower latitudes except 5°S–5°N also meet the needs of an approximately balanced geostrophic relation between Coriolis and pressure forces in meridional direction at great precision, i.e., a semi-geostrophic relationship (Li and Chou 1998). Outside the equatorial belt the geostrophic relation satisfied by zonal winds takes the form

$$fu = -\frac{\partial \phi}{\partial y}, \tag{2.1}$$

indicating that where zonal wind equals zero is where geopotential height is the extremum in meridional direction, with its property dependent on second-order derivative. From (2.1) we have

$$f\frac{\partial u}{\partial y} + \beta u = -\frac{\partial^2 \phi}{\partial y^2}. \tag{2.2}$$

Therefore, at the interface $u = 0$, if $\frac{\partial u}{\partial y} > 0$, meaning west (east) winds to the north (south) of the interface, then we have $\frac{\partial \phi}{\partial y} = 0$ and $\frac{\partial^2 \varphi}{\partial y^2} < 0$, a location for maximum ϕ to be taken meridionally and, likewise, for $\partial u / \partial y < 0$, meaning the easterlies (westerlies) on the north (south) side, one has $\frac{\partial \phi}{\partial y} = 0$ and $\frac{\partial^2 \varphi}{\partial y^2} > 0$, a location for minimum ϕ to be taken in meridional direction. Over the subtropics, as a consequence, the change in position of an easterly-westerly separating line satisfying $u = 0$ and $\partial u / \partial y > 0$ is well indicative of the displacement in location of the SH ridge. By means of this property the characteristic line of $u = 0$ and $\partial u / \partial y > 0$ over subtropics is simply used to investigate the WPSH ridge.

2.3 The vorticity equation

The diagnoses of the SHDR formation are accomplished using the vorticity equation. The pressure-coordinate vorticity equation of the free atmosphere can be given by

$$\frac{\partial \zeta}{\partial t} = \underbrace{-\left(u\frac{\partial \zeta}{\partial x} + v\frac{\partial \zeta}{\partial y}\right)}_{\text{A}} \underbrace{-\omega\frac{\partial \zeta}{\partial p}}_{\text{B}} \underbrace{-\beta v}_{\text{C}} \underbrace{-(f+\zeta)\left(\frac{\partial u}{\partial x} + \frac{\partial v}{\partial y}\right)}_{\text{D}} + \underbrace{\left(\frac{\partial \omega}{\partial y}\frac{\partial u}{\partial p} - \frac{\partial \omega}{\partial x}\frac{\partial v}{\partial p}\right)}_{\text{E}} + \underbrace{R(\zeta)}_{\text{F}}, \tag{2.3}$$

where ζ is the vertical component of relative vorticity (henceforth referred to only as the vorticity), $f = 2\Omega \sin\varphi$ is the Coriolis parameter, and β is the latitudinal gradient of f. Terms A, B, C, D, E, F, and G in the Eq. (2.3) refer to, respectively, the vorticity tendency, the horizontal advection, the vertical advection, the beta term, the divergence,

the twisting or tilting term, and the residual of the sum of the sub-grid scale contributions not accounted for by the synoptic scale variables. A physical description of each term can be found in Fein (1977) or textbook (e.g., Holton 2004).

3. The SHDR event and the related features in July 1998

3.1 The SHDR event

In the summer of 1998 the variations of WPSH are extremely complicated and unusual. One of main characteristics is its abrupt southward withdrawal from the mid-lower valleys of the Yangtze River to the south of South China in middle July (China National Climate Center 1998). To reproduce the retreat process, Fig. 2a shows a time-latitude cross section of the 500 hPa WPSH ridge over 110°–130°E in July. We calculate the average over longitudes of 110°–130°E because the WPSH has the most important impact on the summer weather/climate in China here. As shown in Fig. 2a, the WPSH ridge gradually migrates northward from 26°N to nearly 30°N during July 1–6, followed by the ending of the Mei-yu over the Yangtze-Huai River Valley. On July 14 the ridge undergoes sudden withdrawal southward to 22°N, and then steadily anchors in the vicinity of 20°N. Afterwards, large-scale heavy rainfalls reoccur in the Yangtze River Basin and the second Mei-yu period starts. These processes have been reported in previous studies. However, another interesting phenomenon–SHDRs–appears in Fig. 2a, which has not received any attention before.

The SHDR event occurs during the northward movement and southward "abrupt" retreat of the WPSH in Fig. 2a, which indicates two lines satisfied with $u = 0$ and $\partial u / \partial y > 0$ appear in the north and south, respectively. It is clear that the WPSH is characterized by the single ridge before July 8, while a new ridge occurs at about 17°N on July 8 accompanied by the old ridge at about 30°N. Afterwards, the northern ridge is steadily maintained while the southern one moves northward after a transient retreat. The SHDRs last a few days before the single ridge prevails in the WPSH again. On July 14 only the southern ridge is stable at around 20°N whereas the northern one suddenly disappears. Consequently the ridge of WPSH reconstructs in the south with single-ridge structure after the SHDR event is over. The similar processes could also be clearly seen at 700 hPa (Fig. 2b), but there is a difference that the

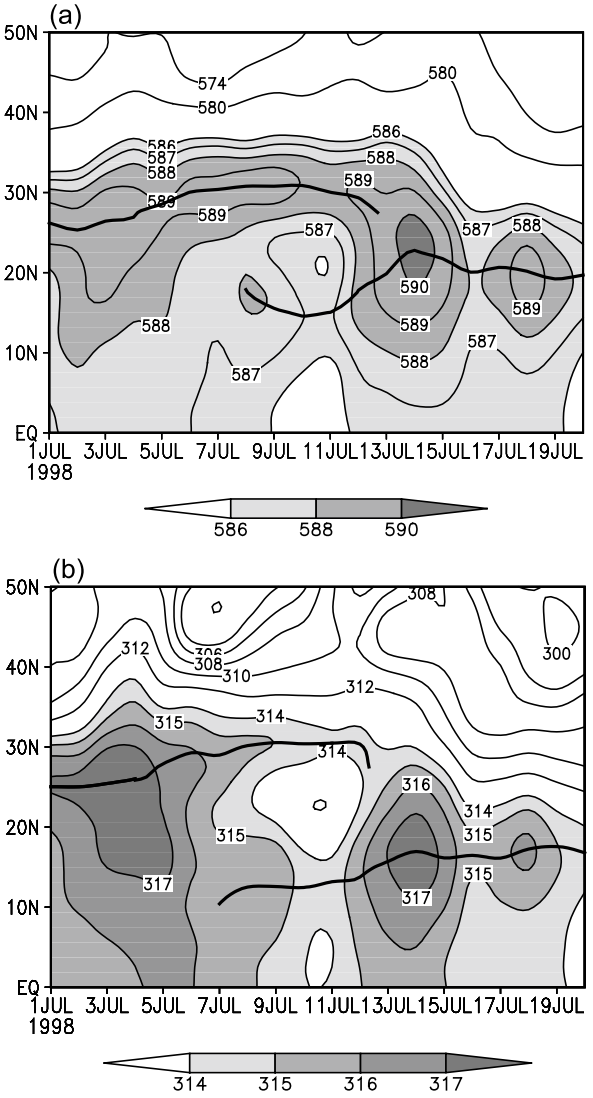

Fig. 2. Time-latitude cross section (110°–130°E) of the daily geopotential height (in dagpm) during July 1–20, 1998 at 500 hPa (a) and 700 hPa (b). The thin solid line stands for the contour of geopotential height, and the thick line for the SH ridge, respectively.

SHDR event at 700 hPa is about one day earlier than that at 500 hPa. Here, we define July 8–13 as the SHDR period according to the observations at 500 hPa because the location of Mei-yu front is related more closely to the WPSH at 500 hPa than that at any other levels.

The above results suggest that the conventional viewpoint of sudden southward withdrawal of the WPSH ridge in middle July 1998 in most of the

previous studies has some limit. In fact, there is a rebuilding process of the WPSH ridge to the south of the original one. As the northern ridge disappears on July 14, the reconstruction ends and the WPSH stays at about 20°N, which finally causes that the Mei-yu event reoccurs over the Yangtze River valley. Therefore, the SHDR event seems to be a precursor signal for the prolonged Mei-yu rain-band in the Yangtze River basin.

3.2 Features related to the SHDRs

In order to explore the basic features of the SHDRs, circulation, temperature and humidity in three periods of July 1–4 (anterior period of SHDRs), July 8–13 (persistence period of SHDRs) and July 14–19 (posterior period of SHDRs) are investigated, respectively. The period of July 5–7 in the diagnosis is missed in order to avoid the possible interference of the equatorial buffer zone[1] with the WPSH in this period.

The 500 hPa mean flow fields with the SH ridge during July 1998 in the three defined phases are displayed in Figs. 3a, 3b and 3c respectively. In the persistence period (Fig. 3b), a subtropical anticyclone (see the thick dashed circle in Fig. 3b) covers over the Western North Pacific (WNP) subtropics meridionally, with its western periphery deformed to great degree. Two WPSH ridges are located at 15° and 30°N, respectively, and the northern one passes through the body of the subtropical anticyclone and joints the SH ridge over the central Pacific. In contrast, the main feature in the anterior and posterior periods of SHDRs as shown in Figs. 3a and 3c is the single-ridge structure of the WPSH, with the small north-south extent of the closed anticyclonic circulation over the WNP subtropics. It should be noted that the double ridges are also found in the west of 110°E in Figs. 3a and 3b, but they will not be further studied since the subject of this study is the double ridges associated with the WPSH. Another distinct feature in Fig. 3 is that in the posterior pe-

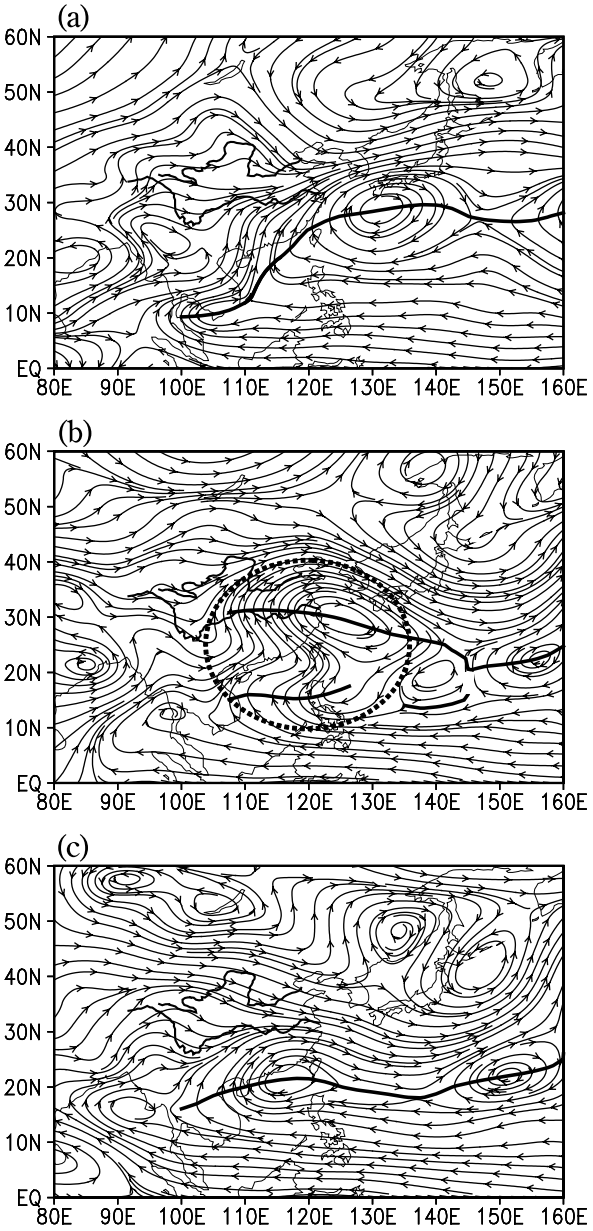

Fig. 3. The 500 hPa mean stream fields during July 1998 for the three periods (a) July 1–4 as the anterior period; (b) July 8–13 as the persistence period; and (c) July 14–19 as the posterior period of double ridges in the Western North Pacific Subtropical High (WPSH). The thick solid lines represent the WPSH ridges, and the thick dashed circle represents the interest area in the persistence period.

1 Equatorial Buffer Zone. This was defined by Conover and Sadler (1960). A buffer zone straddles the equator and separates two oppositely-directed wind streams, the easterly trades and the monsoon westerlies. The sense of rotation in the buffer zone is clockwise in the Northern Hemisphere (NH) summer and anticlockwise in the NH winter. Atkinson, G.D., 1991: *Forecaster's guide to tropical meteorology, Second edition*. URL http://www.weathergraphics.com/dl/tropicalmeteorology.pdf

riod (Fig. 3c) the WPSH ridge is located at about 20°N, much more south than its normal period. This non-seasonal and extraordinary phenomenon may be a result of the reconstruction of the southern ridge as discussed in the previous section.

The vertical circulation structures in the three related periods from the height-latitude cross section along 120°E are further examined (Fig. 4). At this longitude the SHDR event in July 1998 is always typical at any level in the mid-lower troposphere. In the anterior period (Fig. 4a), the WPSH is structured as a single ridge axis that is tilted northward at a small angle with height above 925 hPa. In the neighborhood of the ridge axis, rising (sinking) motions are located above (below) 700 hPa, and a small-scale closed vertical circulation cell exists at 300–150 hPa in the vicinity of 28°N. In the persistence period (Fig. 4b), the salient feature is that two ridge axes co-exist, with one to the south and the other to the north of the ridge axis in the anterior period. The southern ridge appears inside the rising air zone below 400 hPa and tilts northward to great degree with height, while the northern one is located in the sinking zone below 200 hPa and inclines poleward with height above 925 hPa. The northern one is moved about 5 latitudes northward compared with that in the anterior period, and the rising flows at 700–200 hPa turn to a colossal region of subsidence. In the posterior period (Fig. 4c) when the SHDR event is over, the WPSH restores the single-ridge-axis structure with northward incline to even greater degree. Sinking (rising) flows mainly from the middle latitudes are observed (below) above 300 hPa around the axis, which is different from that in the presistence period when the flows are from the low latitudes.

In the previous section, it is apparent that the SHDR system is sufficiently deep and strong as to show up not only at 500 hPa but also throughout the mid-lower troposphere. It is also worth noting that in the anterior and persistence periods of the SHDRs near the ridge axis the flows from the low latitudes prevail while in the posterior period the flows from the middle latitudes are dominant. It suggests that the effects of tropical systems on the WPSH may be very important in the anterior and persistence periods.

Figure 5 presents the 500 hPa mean temperature fields in the anterior, persistence and posterior periods. In the anterior period (Fig. 5a) the temperature field over East Asia–WNP subtropics

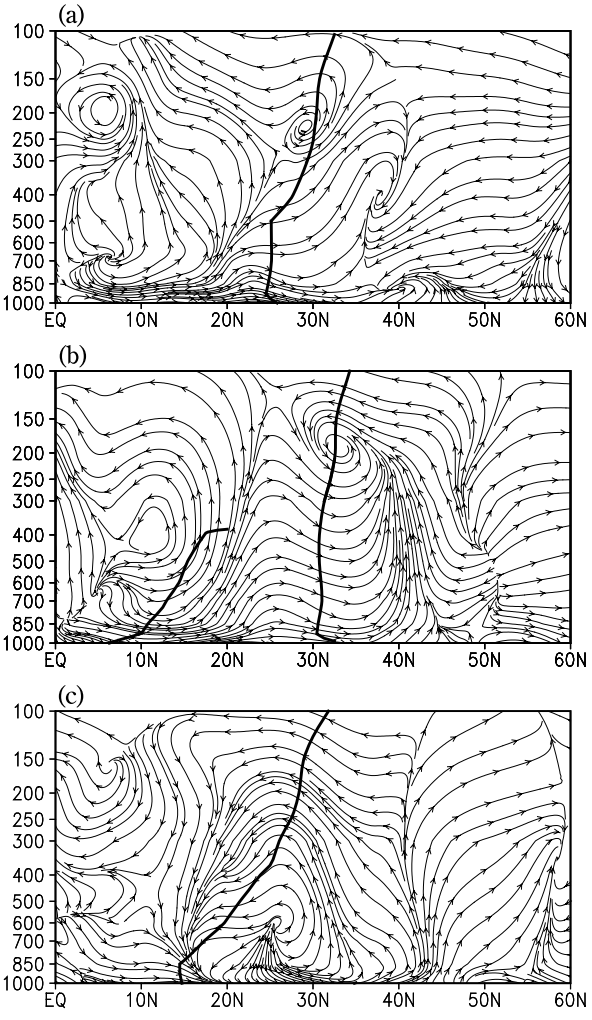

Fig. 4. Height-latitude cross section of mean vertical circulations (v, $-\omega \times 70$) along 120°E for the three periods as Fig. 3. Units: v in m s^{-1}; ω in Pa s^{-1}. The thick solid line represents the SH ridge axis.

displays a warm-cold-warm-cold pattern in the east-west direction with an extensive warm core (its central intensity > 2°C) over the Tibetan Plateau and another weaker one (its central intensity < –5°C) over the ocean to the east of southern and eastern China seaboards. The two cold cores are located over Taiwan and the north-west Pacific to the southeast of Japan, respectively, and the former being weaker in strength than the latter. It is worth mentioning that the warm axis basically lies to the north of the WPSH ridge. In the persistence period (Fig. 5b), the warm core over the Tibetan Plateau weakens and migrates more

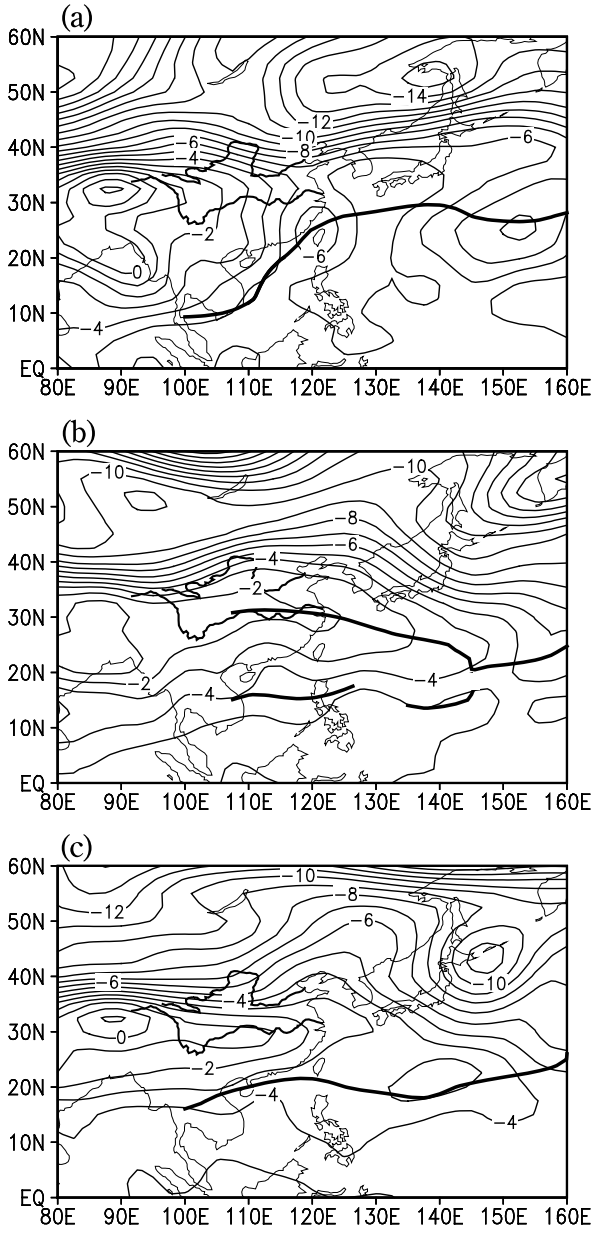

Fig. 5. As Fig. 3, but for the 500 hPa mean temperature fields. Units: °C.

southward than the anterior period, but the warm tongue extends eastward intensively and combines another warm segment. At the same time, the two cold centers are invisible, so that the East Asia–WNP subtropical belt is under the control of an extensive warm zone. The northern ridge coincides with the warm axis. In the posterior period (Fig. 5c) the warm core over the Tibetan Plateau intensifies again and covers an enlarged area, with the –4°C isoline extending eastward as far as 160°E. The warm axis remains to the north of the ridge although the WPSH is inside a large-scale warm area.

According to these results, the configurations of temperature and pressure fields in the anterior and posterior periods are consistent with the traditional viewpoint that the warm ridge axis below 200 hPa is located mainly on the poleward side of the WPSH ridge axis. In the persistence period, however, the coincidence of the northern ridge with the warm axis is distinct. According to the thermal wind relation, such distribution that the slope of the northern ridge axis with height (Fig. 4b) is very small in the persistence period may be related to above allocation between temperature and pressure fields.

Figure 6 presents relative humidity (RH) at 500 hPa in the three periods. Generally, the 500 hPa RH over land with dense isopleths is much higher than that over seas, and the body area of WPSH corresponds to a dry zone, with its ridge going through the center of the zone. In eastern Asia, the maximum RH axis is situated about 10 latitudes north of the SH ridge, roughly corresponding to the location of rainbelt over the area. Particularly in the presistence period (Fig. 6b), another maximum RH zone occurring between the southern and northern ridges is a special characteristic for SHDRs. At the same time, the southern ridge is located in the wetter area than the northern ridge. The possible reason is that the southern ridge and tropical convection discussed in section 5 bring the water vapor and cause the rising motion in that area.

4. Generation and development of the SHDR event

Since the southward stagnancy of the WPSH in middle of July 1998 results from the reconstruction of the WPSH ridge associated with the SHDR event, the SHDR event can be regarded as the precursor signal for the onset of the second Meiyu over the Yangze River valley. In this section, we try to discuss why the southern ridge generates and how it persists.

4.1 Evolution of vorticity fields during the SHDR event

Figure 7 displays the time-latitude cross sections of daily relative vorticity averaged over 110°–130°E at 500 hPa and over 120°–140°E at 850

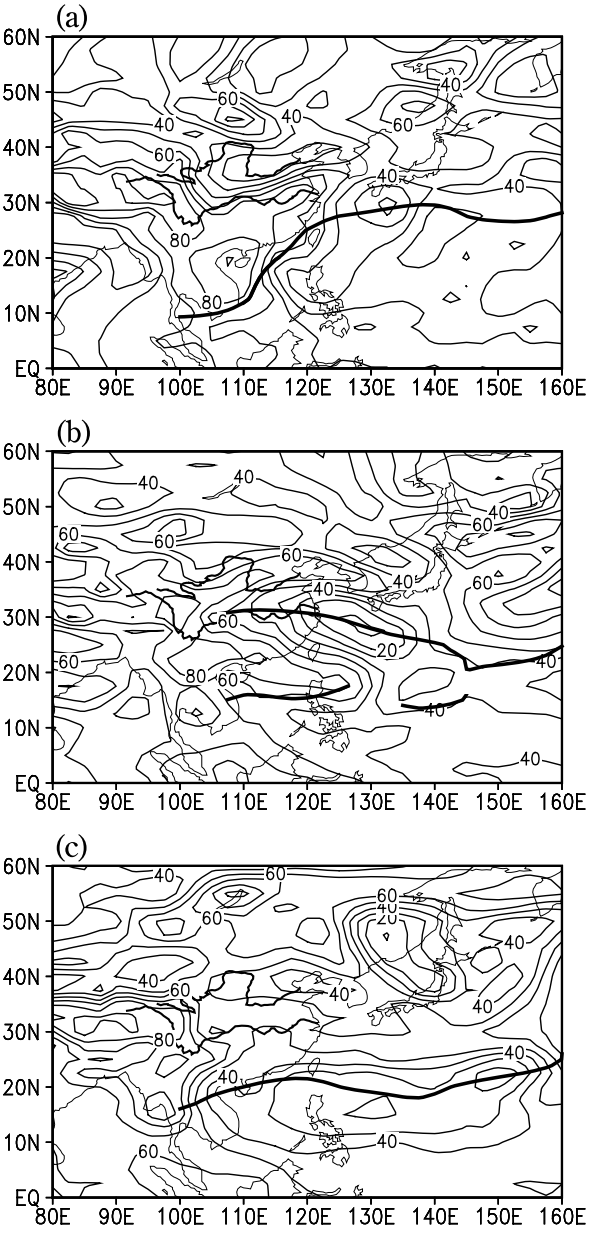

Fig. 6. As Fig. 3, but for the 500 hPa mean relative humidity fields. Units: %.

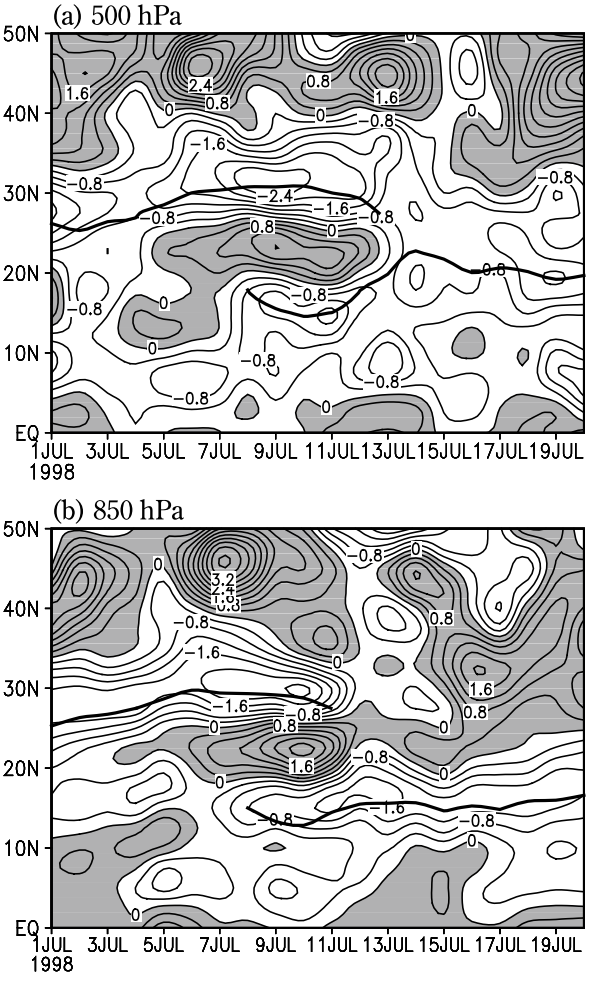

Fig. 7. As Fig. 2, but for the relative vorticity (in 10^{-5} s^{-1}) distributions averaged (a) over 110°–130°E at 500 hPa and (b) over 120°–140°E at 850 hPa. The shaded area stands for positive relative vorticity, thin solid line for vorticity contour, and thick solid line for the WPSH ridge, respectively.

hPa during July of 1998. At 500 hPa (Fig. 7a) a negative-positive-negative vorticity train can be seen from the south to north over the tropics and subtropics before July 13. The northern vorticity moves northward with time and reaches its maximum on July 9, followed by a dramatic decline. The south side of the negative vorticity is a positive vorticity zone, which is seen between 10° and 15°N on July 4 and between 20°–25°N on July 6. Afterwards, the positive vorticity intensifies, and reaches its maximum during July 9–11. Two days later, the positive vorticity zone disappears. On the other hand, a negative vorticity band centered at 7.5°N occurs during July 3–7, thereafter its center jumps rapidly to 15°N and the southern ridge appears simultaneously. After July 13 the northern ridge disappears and an extensive region between 5°–30°N exhibits negative vorticity. These processes are clearly presented at 850 hPa (Fig. 7b). At the beginning the positive vorticity

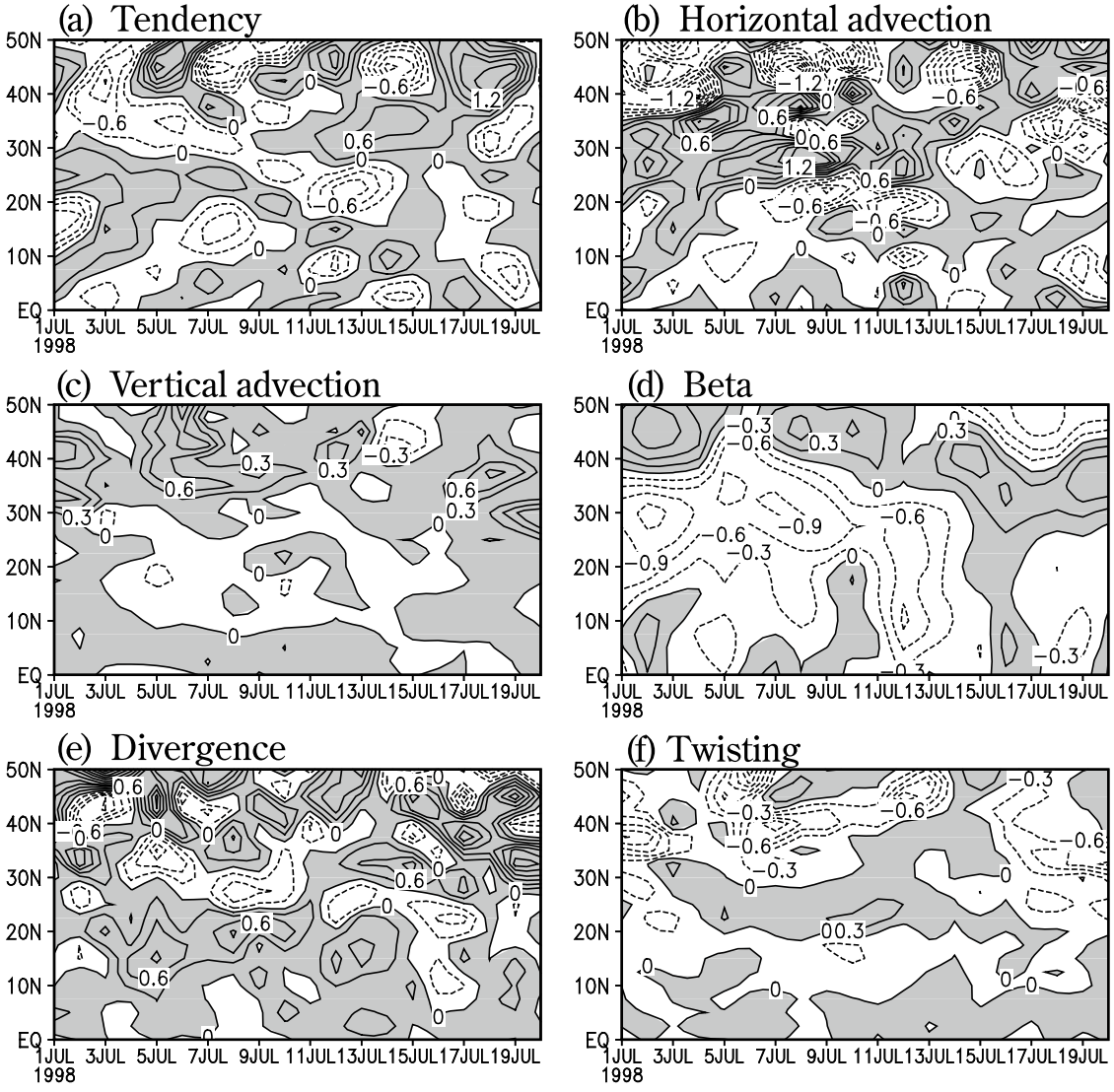

Fig. 8. As Fig. 2, but for the daily 500-hPa vorticity equation terms. (a) Vorticity tendency; (b) Horizontal vorticity advection; (c) Vertical advection; (d) Beta term; (e) Divergence; (f) Twisting term. Contour interval is 0.3×10^{-10} s^{-2}. The positive vorticity is shaded.

area emerges to south of 10°N and subsequently migrates northward to 12°N on July 5, while its center suddenly jumps to 22°N on July 6. At the same time, the center of negative vorticity suddenly moves northwards to about 15°N from the south of 5°N which appears on July 3, hereafter both the positive and negative vorticity bands are being maintained.

4.2 The diagnoses of the vorticity equation during the SHDR

The vorticity equation will be used to diagnose the dynamic process of the SHDRs in this section. In brief, the ensuing map-based discussion will focus on the origin and maintenance of the southern negative vorticity associated with the southern ridge averaged over 110°–130°E at 500 hPa.

Figure 8 presents the vorticity tendency and contributions of each term on the right-hand side of Eq. (2.3). The magnitude of each term is shown as 10^{-10} with units of s^{-2}. First, the vorticity tendency term (Fig. 8a) is examined. On July 1 negative vorticity tendency appears near the equator. Afterwards it moves northward with time,

and reaches the first extremum at about 3°N on July 3, the second one at about 7°N on July 5, and the third one at about 15°N on July 7–8. The processes correspond to the intensification and northward movement of the southern negative vorticity in Fig. 7a. It can also be seen that the positive vorticity tendency on the south and north sides of the negative vorticity tendency moves northward, which corresponds to the intensification and northward movement of the positive vorticity between two ridges in Fig. 7a. After July 10, the positive vorticity tendency at 18°–28°N gradually turns to negative vorticity tendency, while the positive vorticity tendency at 28°–40°N gradually intensifies. The former corresponds to the weakening and disapperance of the positive vorticity, and the latter accompanies to the weakening and disapperance of the northern negative vorticity associated with the northern ridge. Through examining the terms on the right side of Eq. (2.3), the effects on the variations of the vorticity tendency are explored. As shown in Figs. 8b–8f, horizontal advection and beta term are dominant factors to influence on the southern negative vorticity with horizontal advection contributing the most, and the divergence and horizontal advection terms play a crucial role in the emergence and development of the positive vorticity between the two WPSH ridges. In addition, divergence, horizontal advection and beta term together contribute to the weakening and disappearence of the positive vorticity and northern negative vorticity. The remaining terms have no significant effect.

The diagnosis indicates that the origin of the southern ridge may be associated with the northward movement of the southern negative vorticity determined by horizontal advection and beta term, while the maintenance of the SHDR event may be related to the evolution of positive vorticity from the lower latitudes contributed by divergence and horizontal advection. As early as the late 1960s, the effect of equatorial anticyclone on the SH has been analyzed in detail by Fujita (1969) and later by Sadler (1971), whose results have indicated that the formation, development and westward movement of equatorial anticyclone over the eastern equatorial Pacific can cause the SH over the Pacific to retreat southwards. In addition, the convection over the tropical WNP may be considered as a crucial factor influencing the WPSH meridional movement, since it acts as a major heating source (Nitta 1987; Huang et al. 2004). Therefore, the question is whether the negative and positive vorticities are related to the equatorial anticyclone and the tropical convection.

4.3 Effect of equatorial buffer zone on the genesis of the SHDR

Figure 9 presents the 500 hPa daily stream fields and horizontal advection in the vorticity equation during July 5–8. Although both horizontal advection and beta term dominate the southern negative vorticity, the effect of beta term can be implied in stream fields because the sign of beta term depends on the southerlies. On July 5 the strong subtropical anticyclonic circulation stands over the WNP with its center at the point of (132.5°E, 30°N) in Fig. 9a. An equatorial anticyclone is located over the western South China Sea, tending towards SW-NE, meanwhile, an equatorial buffer zone over the south of the Philippines. The negative vorticity advection is located to southwest of the equatorial buffer zone with the center in 110°–150°E, which helps the buffer zone to extend westward and the equatorial anticyclone to expand southeastwards. On July 6 the subtropical anticyclone snails northwards in Fig. 9b. The equatorial anticyclone stretches meridionally, and the equatorial buffer zone intensifies and extends westwards. At this time, the strong negative vorticity advection is still located to south-west of the equatorial buffer zone, which contributes to the further westward extension of the buffer zone and the further south-east expanding of the equatorial anticyclone. On July 7 the equatorial anticyclone merges with the equatorial buffer zone in Fig. 9c, accompanying with a greatly expansion westward of the circulation in the south of the WPSH. Another important feature is that the strong negative vorticity advection occurs from the eastern Indo-China Peninsula to the western Pacific via South China Sea. In addition, the negative contribution of beta term is large from the east of South China Sea to the north of the Philippines according to the stream field. Thus, both horizontal advection and beta term provide the coherent contribution for the northward movement of the equatorial anticyclone. One day later (Fig. 9d), the equatorial anticyclone rapidly moves northwards until it merges into the WPSH. It follows that a new high ridge bulids up in the south of the WPSH and the SHDR event occurs.

The combination process of the equatorial anticyclone and the WPSH is clearer when examining

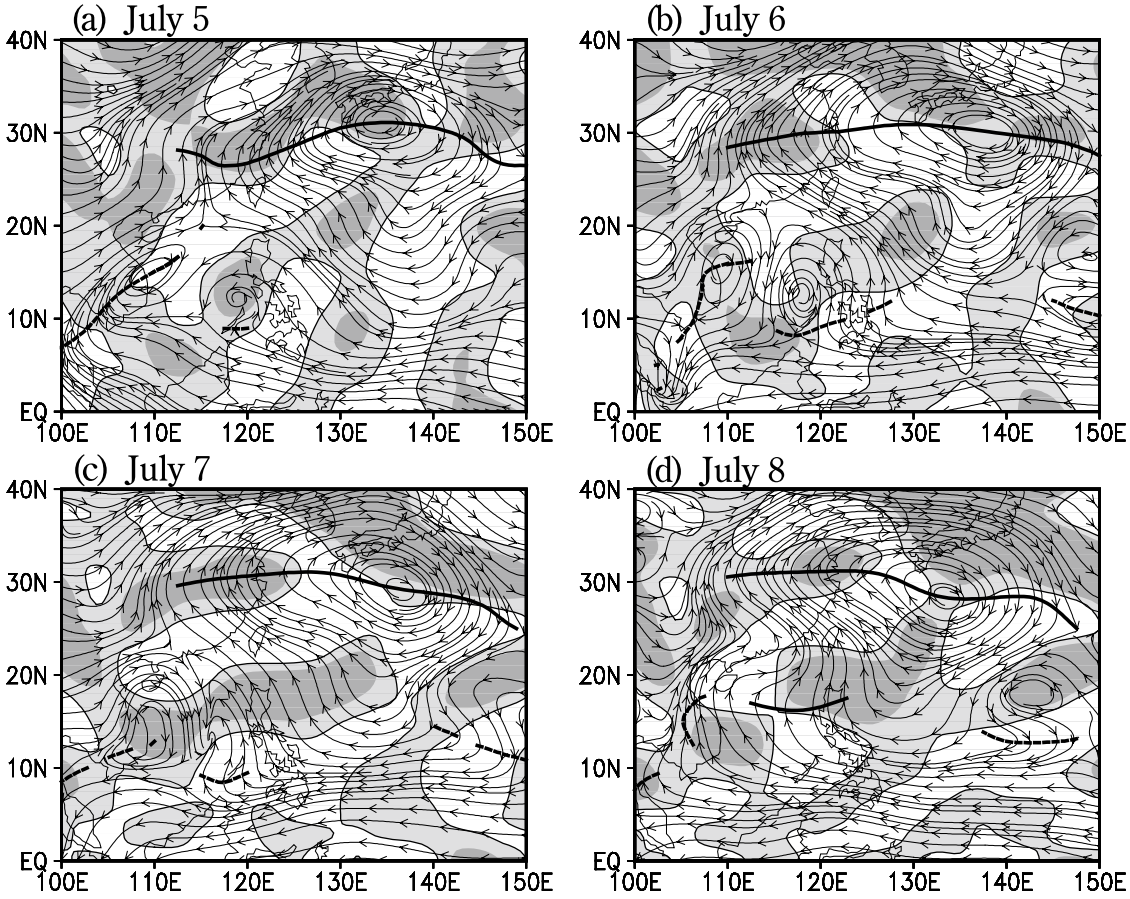

Fig. 9. The 500 hPa daily stream fields and the horizontal advection term in the vorticity equation on (a) July 5; (b) July 6; (c) July 7; (d) July 8, 1998. The heavy solid lines stand for the SH ridges, and the thick dashed lines for the ridges of equatorial anticyclone. Shaded areas are the negative vorticity contributions, and darker shaded areas are the negative vorticity contributions less than -0.5×10^{-10} s^{-2}

the daily height-latitude cross sections of zonal wind along 120°E during July 1998 (Fig. 10). Figure 10a shows that three ridge axes exist in the vertical field on July 7, with the first at 27°–35°N extending from the surface to the tropopause, the second at 15°–20°N in higher troposphere (400–150 hPa), and the third at around 10°N and in the lower troposphere (below 600 hPa). From the geopotential height and stream fields (figures omitted), the first and second ridge axes are associated with the SH ridge axes while the third one is related to the ridge axis of the equatorial anticyclone. On July 8 (Fig. 10b), the ridge axis of the equatorial anticyclone in the lower troposphere rapidly moves northwards and extends upwards and combines with the SH ridge axis in the higher troposphere, with a result that a SH ridge axis occurs from the surface to 150 hPa. At this time, the northern SH ridge axis changes little, and a structure with the WPSH double ridge axes is formed. On July 14 (Fig. 9c), the WPSH turns back to a single-ridge-axis structure, and its ridge axis rapidly inclines northwards with height.

The results above suggest that the equatorial anticyclone moving northwards and merging with the WPSH may be one of the important reasons of the genesis of the double ridges, which is consistent with the previous studies (Fujita 1969; Sadler 1971) to some degree. The results, however, also demonstrate another different phenomenon that the WPSH does not rapidly withdraw southwards after the mergence of the equatorial anticyclone with the WPSH, but the northern and southern ridges coexist for 6 days. It suggests that there is

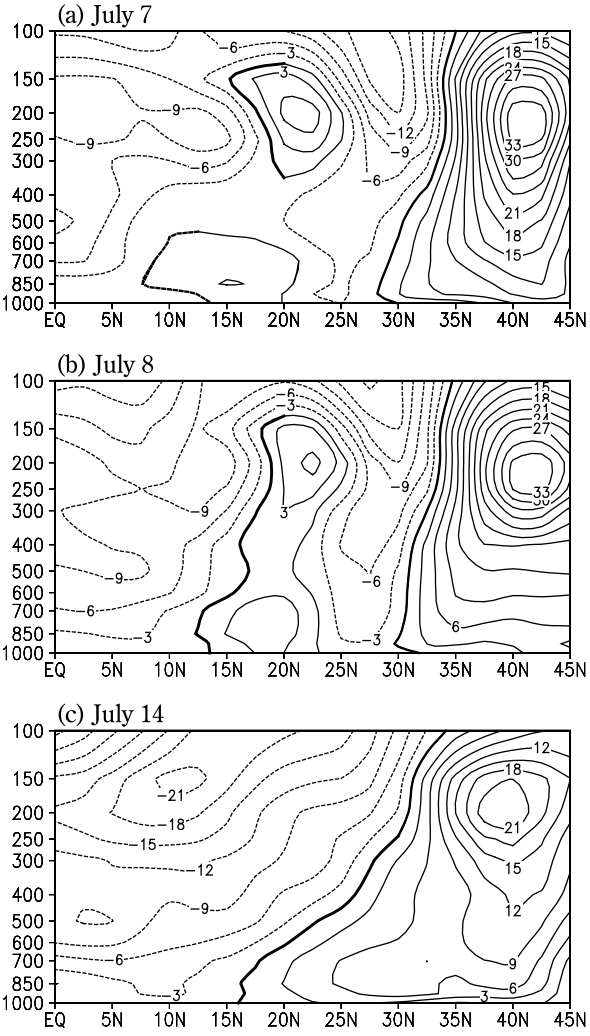

Fig. 10. Height-latitude cross sections of daily zonal wind along 120°E on (a) July 7; (b) July 8; (c) July 14, 1998. The thick solid line denotes the WPSH ridge axis, and the thick dashed line for the ridge axis of equatorial anticyclone.

another factor responsible for the maintenance of the SHDRs. The evolution of positive vorticity is investigated to identify such factor.

4.4 Influence of tropical convection on the genesis and development of the SHDRs

TBB distribution can reflect, to a fairly great extent, the circulation systems at mid and lower latitudes. Low-value TBB regions are generally cloudy ones and their cores indicate severe convection centers (Muramatsu 1983; He et al. 1997).

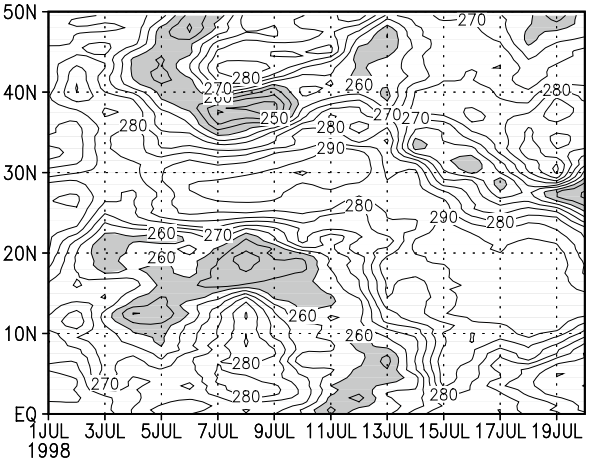

Fig. 11. As Fig. 2, but for daily TBB (Units: °K). The values less than 260°K are shaded.

To better understand the evolution of positive vorticity at mid- and lower latitudes, time-latitude cross section (110°–130°E) of the daily TBB in July is shown in Fig. 11. On July 3, the tropical convection occurs at about 12°N, and then moves northwards due to the positive vorticity advection to the north with the minimum on July 4–5. This corresponds to the positive vorticity at 10°–15°N in Fig. 7a quite well. Afterwards, the convection continues to move northwards and arrives at another minimum on July 8, which is consistent with the northward movement and the maximum on July 9 of the positive vorticity. On July 11, the minimum band of TBB disappears after maintaining for two days. At this time, the positive vorticity weakens rapidly. Gill (1980) pointed out that the diabatic heating triggered by tropical convection located to north of the equator produces the strong upward motion and a low to the north-west flank of the heating region itself. The above well correspondence may be related to the strong convergence triggered by the convection as demonstrated in the divergence term of the vorticity equation in Fig. 8e. It suggests that the tropical convection may play a very important role in the SHDR event because it prevents the northern ridge from withdrawing southwards and the southern one from advancing northwards.

In conclusion, the genesis of the southern ridge is closely related to the northward movement of the equatorial anticyclone (equatorial buffer zone), and the maintenance of the SHDRs is likely due to

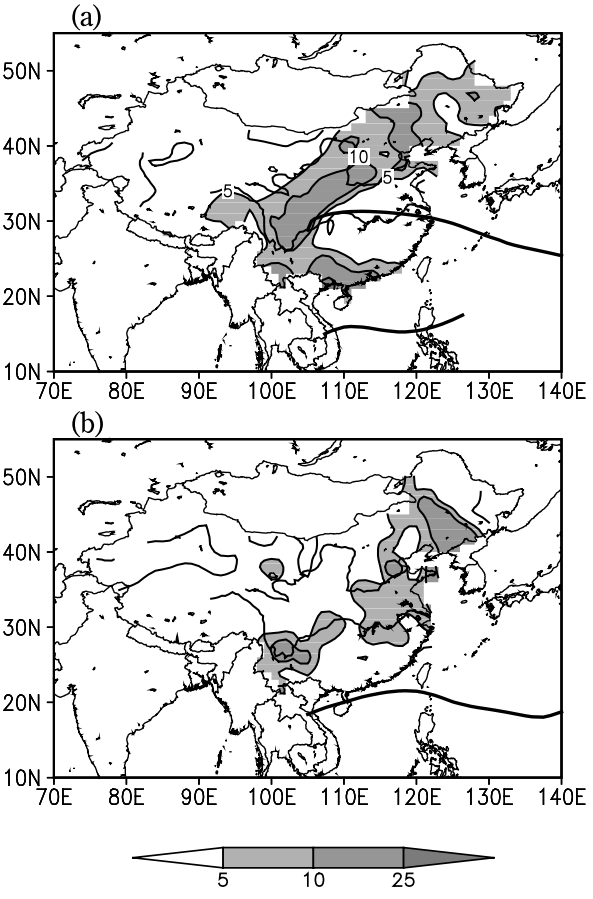

Fig. 12. The patterns of mean rainfall during July 1998 in (a) the WPSH double-ridge case (July 8–13) and (b) the WPSH single-ridge case (July 14–19) in China. The thick solid line signifies the WPSH ridge line. Units: mm/day.

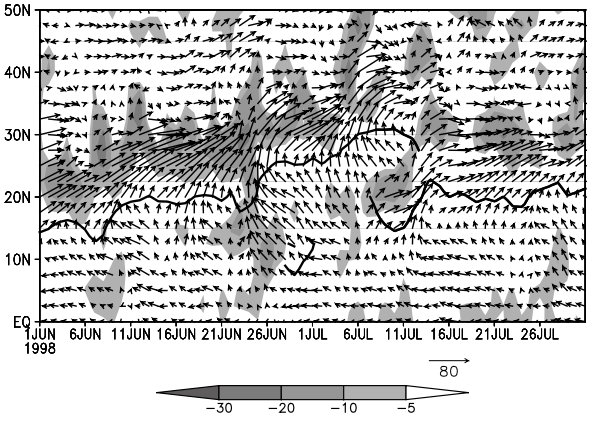

Fig. 13. As Fig.2, but for the vapor flux vectors (shown as arrows, units: 10^{-1} kg m^{-1} s^{-1}) and vapor flux divergence (units: 10^{-7} kg m^{-2} s^{-1}; shaded areas for $< -5 \times 10^{-7}$ kg m^{-2} s^{-1}) integrated from 1000 to 300 hPa during June–July 1998. The solid lines denote the WPSH ridges.

the effect of tropical convection.

5. Possible effects of the double-ridge persistence on the rainfall pattern in eastern China

It is well recognized that the ridge of WPSH usually determines the location of the rainband from the cases of the single ridge in WPSH (Tao and Chen 1987; Ding 1994; Ninomiya 2004). What effect does the SHDRs have on the rainfall pattern in eastern China?

Figure 12 presents the patterns of rainfall over China in the persistence and posterior periods of the SHDRs during July 1998. In the presistence period (Fig. 12a), two rainbelts exist as an italic "*L*"-like pattern along the paths of the ridges. One comes from the upper-mid reaches of the Yangtze River, extending northeastward across the upper-mid valleys of the Yellow River and Huai River into northeast China, and another stretches southeastwards and covers South China. This pattern differs greatly from the single ridge cases of WPSH (Fig. 12b) in which only a rainbelt exists to the north of SH, originating from the Yangtze River Valley to northeast China in northeast direction.

Figure 13 presents a time-latitude cross section of vapor transport vectors and flux divergence integrated from surface to 300 hPa. It is apparent that during the single ridge of WPSH a high-value vapor transport belt from the southwest is always located to the north of the WPSH ridge. This is due to that the anticyclonic circulation of WPSH can lead the abundant water vapor over the Bay of Bengal and South China Sea into East Asia. As a result, it provides a good supply of water vapor for the persistence of a rainfall pattern there, which is basically in agreement with the previous statement. During the double ridges, however, apart from the above high-value transport band, another vapor band from the southwest emerges between the two ridges and just corresponds to the rainbelt over South China. It seems that the double-ridge coexistence alters the original vapor transferring mode associated with the single-ridge case so that the vapor transports along two paths. It facilitates

the appearance and persistence of two rain belts to the north of each ridge.

6. Summary and discussion

This study is devoted to re-investigation of the anomalous activities and evolutions of the WPSH during the breaking of the Mei-yu season in the summer of 1998. Two new facts are found. One concerns the reconstruction of the WPSH ridge in the south. It contributes to the stagnancy of WPSH in the south in middle of July and is different from the previous view of the sudden southward displacement of the original ridge. The other is the proposal of the concept of the SHDRs that two ridges coexist in the WPSH. It should be noted that the facts are not limited in the NCEP data we utilized, but also clear in the ECMWF reanalysis data (figure not shown).

The structures of double ridges show the northern ridge has coherent characteristics with the traditional single ridge, while the southern ridge is characterized by the tropical systems. It might be related to the fact that in the forepart of SHDR period the southern WPSH is weaker than the northern and apt to be influenced by the tropical systems as shown in the geopotential height field (Fig. 2) and the relative vorticity distribution (Fig. 7). Vorticity evolution and the diagnoses of vorticity equation indicate that the formation and maintenance of the SHDRs are associated with the emergence and reinforcement of the positive and negative vorticity cores of low-latitude origin. The former is closely related to the equatorial anticyclone moving northward and merging with the WPSH, and the latter is associated with tropical convections.

As indicated in the previous studies, the ridge of WPSH usually determines the location of the rainband. Our analysis demonstrates that the double-ridge coexistence alters the original vapor transferring mode associated with the single-ridge case so that the vapor transports along two paths. It seems to facilitate two rainbelts in eastern China shaped as an italic "*L*"-like pattern.

The capability to correctly predict the sudden variations of the WPSH and the onset of the second Mei-yu is a challenging problem with very significant implications for society given the flood impacts. The SHDR phenomenon provides the precursor signal for them, and can improve our forecasting capability to some degree. However, more observational and modeling case studies need to be performed to generalize the conclusions above. In particular, some efforts should be made to understand the effect of SHDRs on the abnormal variations of the WPSH and intrinsic relationship between SHDRs and rainfall patterns.

Acknowledgements

The authors would like to thank Profs. Guoxiong Wu and Yimin Liu for their constructive suggestions that led to much improvement on this paper. We also thank Drs. Yonghui Lei, Min Wen, Ming Ying, Jinghui Yan for their kind assistance. The study is jointly supported by the Natural Science Foundation of China (NSFC 40475021), 973 program (2006CB403600), and NSFC 40523001.

References

China National Climate Center, 1998: *China severe flood and climate anomaly*. Meteorological Press, Beijing, 4–30 (in Chinese).

Ding, Y.H., 1994: *Monsoons over China*, Kluwer Academic Publishers, Dordrecht/Boston/London, 419 pp.

Ding, Y.H. and Y. Liu, 2001: Onset and the evolution of the summer monsoon over the South China Sea during SCSMEX Field Experiment I 1998. *J. Meteor. Soc. Japan*, **79**, 255–276.

Ding, Y.H., Y. Zhang, Q. Ma, and G.Q. Hu, 2001: Analysis of the large-scale circulation features and synoptic systems in East Asia during the intensive observation period of HUBEX/GAME. *J. Meteor. Soc. Japan*, **79**, 277–300.

Fein, J.S., 1977: Global vorticity budget over the tropics and subtropics at 200 mb during the northern hemisphere summer. *PAGEOPH*, **115**, 1493–1500.

Fujita, T.T., K. Watanabe, and T. Izawa, 1969: Formation and structure of equatorial anticyclone caused by large-scare cross-equatorial flows determined by ATS-1 photographs. *J. Appl. Meteor.*, **8**, 649–667.

Gerald D. Bell, Michael S. Halpert, Vernon E. Kousky, Melvyn E. Gelman, Chester F. Ropelewski, Arthur V. Douglas, and Russell C. Schnell, 1999: Climate Assessment for 1998. *Bull. Amer. Meteor. Soc.*, **80**, 1040–1040.

Gill, A., 1980: Some simple solutions of heat-induced tropical circulation. *Quart. J. Roy. Meteor. Soc.*, **106**, 447–462.

He, J.H., Q.G. Zhu, and M. Murakami, 1997: TBB data-revealed features of Asian-Australian monsoon seasonal transition and Asian summer monsoon establishment. *J. Trop. Meteor.*, **3**, 18–26.

Holton, J. R., 2004: *An Introduction to Dynamic Meteorology, 4th Edition*. San Diego: Academic Press,

535 pp.

Huang, R.H., G. Huang, and Z.G. Wei, 2004: Climate variations of the summer monsoon over China. *East Asian Monsoon*, C.-P. Chang, Ed., World Scientific Publishing, Singapore, 213–270.

Huang, S.S. and M.M. Tang, 1962: Some signatures and implication of the meridional shift in position of subtropical highs in a year. *J. Nanjing Univ.* (Edition of Meteorology), **2**, 41–56 (in Chinese).

Kalnay, E. and Coauthors, 1996: The NCEP/NCAR 40-Year Reanalysis Project. *Bull. Amer. Meteor. Soc.*, **77**, 437–471.

Krishnamurti, T.N., 1979: Tropical Meteorology, *Compendium of Meteorology II*. WMO-No. 364, World Meteorological Organization, 428 pp.

Kurihara, K., 1989: A climatological study on the relationship between the Japanese summer weather and the subtropical high in the western northern Pacific. *Geophys. Mag.*, **43**, 45–104.

Li, J.P. and J.F. Chou, 1998: Dynamical analysis on splitting of subtropical high-pressure zone—Geostrophic effect. *Chinese Sci. Bull.*, **43**, 1285–1288.

Muramatsu, T., 1983: Diurnal variations of satellite measured TBB areal distribution and eye diameter of mature typhoon. *J. Meteor. Soc. Japan*, **61**, 77–90.

Ninomiya, K., 1984: Characteristics of Baiu front as a predominant subtropical front in the summer Northern Hemisphere. *J. Meteor. Soc. Japan*, **62**, 880–894.

Ninomiya, K., 2004: Large and mesoscale features of Baiu front associated with intense rainfalls. *East Asian Monsoon*, C.P. Chang, Ed., World Scientific Publishing, Singapore, 404–435.

Nitta, T., 1987: Convective activities in the tropical western Pacific and their impact on the northern hemisphere summer circulation. *J. Meteor. Soc. Japan*, **65**, 373–390.

Sadler, J.C., 1971: Forecasting minimum cloudiness over the Red River Delta during the summer monsoon. *Forecaster's Guide to Tropical Meteorology*, Atkinson, G.D., Ed., USAF Air Weather Service, Technical Report No. 240, 364 pp.

Sadler, J.C., 1975: The upper tropospheric circulation over the global tropics, *Technical Report UHMET* 75–05, Dept. of Meteorology, Univ. Hawaii, Honolulu, Hawaii, 35 pp.

Tao, S.Y. and L.X. Chen, 1987: A review of recent research on the East Asian summer monsoon in China. *Monsoon Meteorology*, C.P. Chang and T.N. Krishnamurti, Eds., Oxford Univ. Press, New York, 60–92.

Tao, S.Y. and F.K. Zhu, 1964: Variation of summer circulation pattern at 100 hPa over South Asia and its relation with the movement of the subtropical high over western Pacific (in Chinese), *Acta Meteological Sinica*, **34**, 385–394.

Wang, B. and T. Li, 2004: East Asian monsoon-ENSO interactions. *East Asian Monsoon*, C.P. Chang, Ed., World Scientific Press, Singapore, 177–212.

Wang, W.C., W. Gong, and H.L. Wei, 2000: A Regional Model Simulation of the 1991 Severe Precipitation Event over the Yangtze-Huai River Valley. Part I: Precipitation and Circulation Statistics. *J. Climate*, **13**, 74–92.